

Effect of Cerium Precursor in the Synthesis of Ce-MCM-41 and in the Efficiency for Liquid-Phase Oxidation of Benzyl Alcohol

Carlos M. Aiube^{1*}, Karolyne V. de Oliveira² and Julio L. de Macedo^{1*}

¹ Group of New Materials for Sustainable Chemical Catalysis, University of Brasília, Institute of Chemistry, Campus Darcy Ribeiro, 70910-900, Brasília-DF, Brazil.

² Laboratory of Materials and Fuels, University of Brasília, Institute of Chemistry, Campus Darcy Ribeiro, 70910-900, Brasília-DF, Brazil.

* Correspondence: carlos.unb12@gmail.com (C. M. A.) and julio@unb.br (J. L. M.); Tel.: +55-61-3107-3877 (J. L. M.).

FIGURES

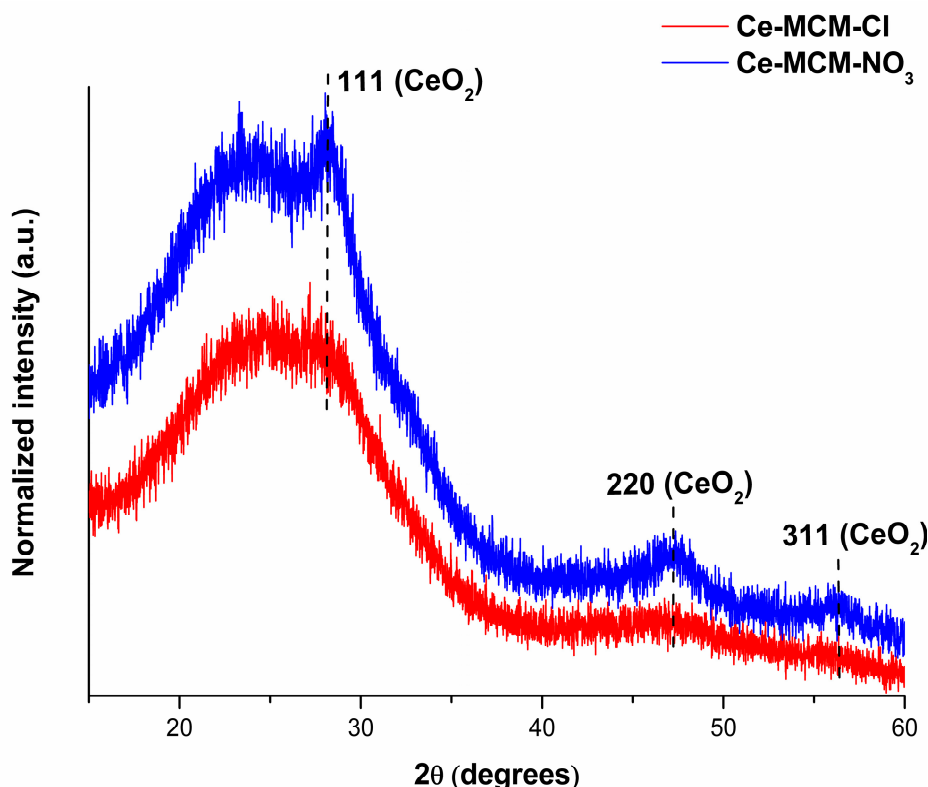


Figure S1. XRD patterns of Ce-MCM-Cl and Ce-MCM-NO₃ materials at high angle region.

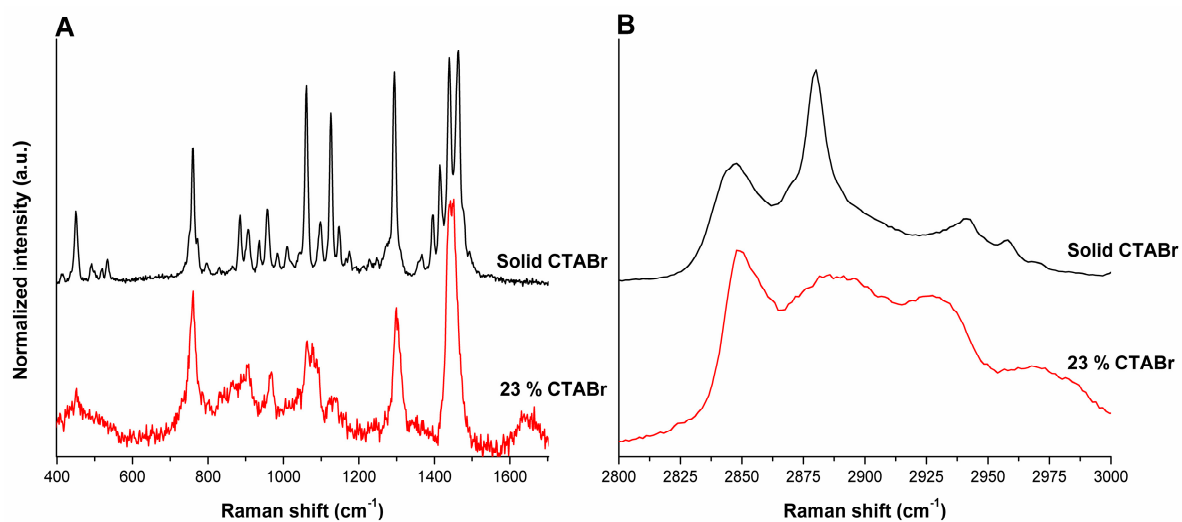


Figure S2. Raman spectra of CTA⁺ systems between 400 - 1700 cm⁻¹ (A) and 2800 - 3000 cm⁻¹ (B).

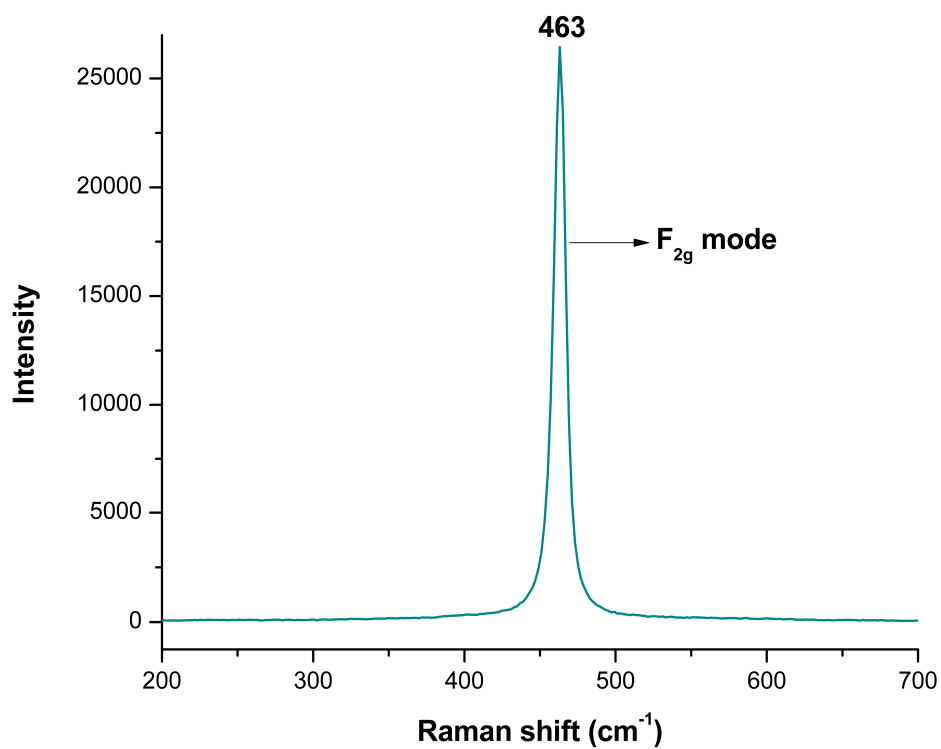


Figure S3. Raman spectrum of crystalline CeO₂.

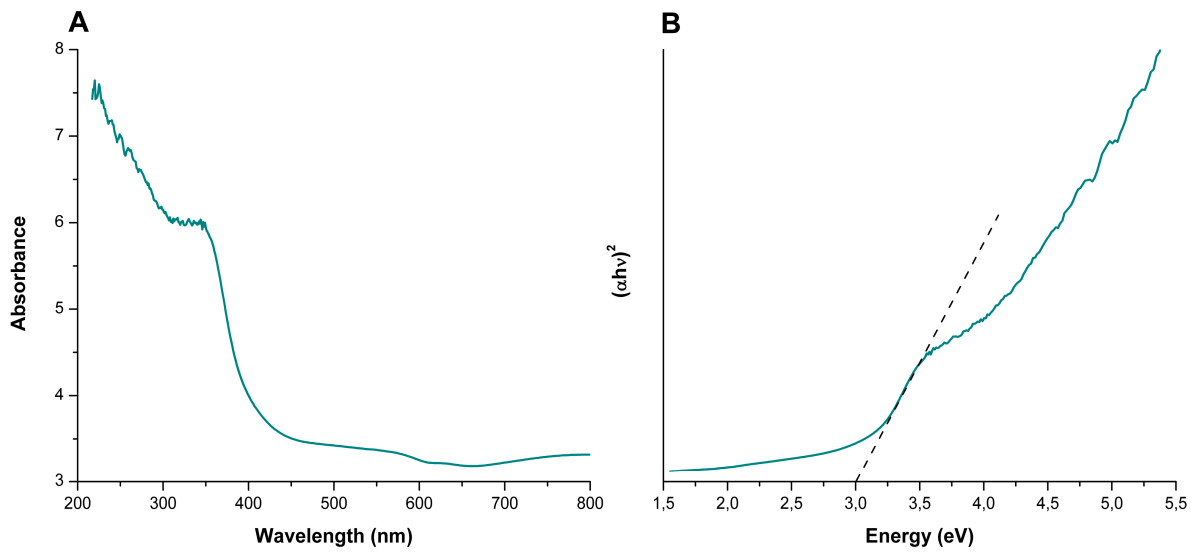


Figure S4. Absorption spectra (A) and Davis-Mott plot (B) for of CeO₂.

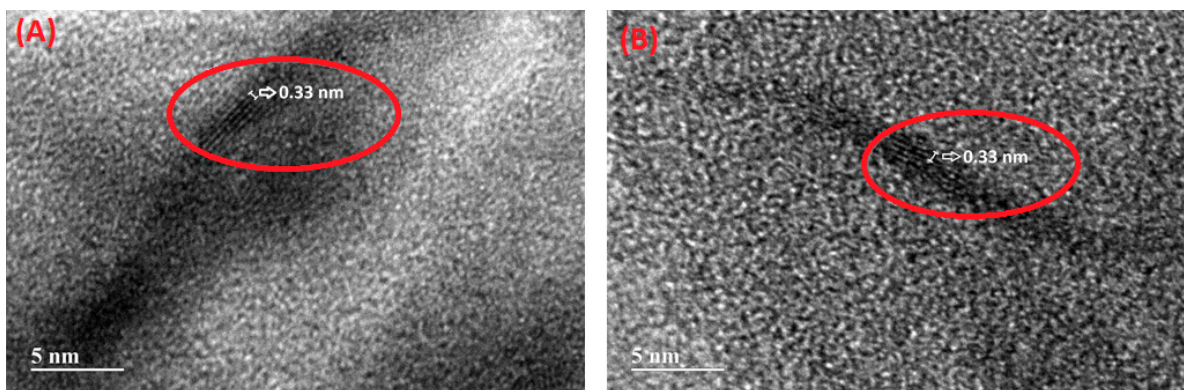


Figure S5. High magnification in HRTEM images highlighting CeO₂ 110 interplanar spacing for: Ce-MCM-Cl (A) and Ce-MCM-NO₃ (B).

TABLES

Table S1. Raman band assignments for CTA⁺ cations in as-synthesized MCM-41 materials and template standards [50,53,54].

Raman shifts (cm ⁻¹) for observed bands					Assignment
Solid CTABr	23 wt.% CTABr	A-Si-MCM-41	A-Ce-MCM-Cl	A-Ce-MCM-NO ₃	
450	452	446			longitudinal accordion mode
492		510			longitudinal accordion mode
520					longitudinal accordion mode
534					longitudinal accordion mode
761	761	761	761	757	CH ₃ rock from N(CH ₃) ₃
773					CH ₃ rock from N(CH ₃) ₃
885					terminal CH ₃ rock
906	908	910	911	913	v _s C-N ⁺
936					v _a C-N ⁺
957	968	964	968	964	CH ₂ rock
983					CH ₂ rock
1011					CH ₂ rock
1045	1041	1041	1040	1039	CH ₂ twist
1061	1063	1061	1063	1063	v _s C-C + CH ₂ wag
	1076	1076	1076	1076	v _s C-C gauche
1098					v _s C-C, crystalline
1126	1122	1120	1122	1120	v _a C-C + CH ₂ wag
	1140	1135	1138	1134	v _a C-C gauche
1175					CH ₂ wag, crystalline
1213					CH ₂ wag, crystalline
1228					CH ₂ wag, crystalline
1247					CH ₂ wag, crystalline
1294	1299	1299	1299	1296	CH ₂ twist
1367					δ _s C-CH ₃
1395					δ _s C-H from N(CH ₃) ₃
1415					δ _s C-H from CH ₂ , crystalline
1439	1443	1449	1449	1448	δ C-H from CH ₂
1464					δ _a C-H from CH ₂ , crystalline
2848	2848	2849	2851	2848	v _s C-H from CH ₂
2880	2885	2884	2884	2887	v _s C-H from CH ₂
2941	2928	2923	2920	2920	v _a C-H from CH ₃
2958	2968	2966	2965	2966	v _a C-H from CH ₃

Table S2. TGA results for the as-synthesized MCM-41 materials.

Sample	Temperature range (°C)	Mass loss (%)	DTG maximum (°C)	CTA ⁺ /SiO ₂ ratio
A-Si-MCM-41	R.T.-129	6.27	61	0.163
	129-270	23.32	248	
	270-322	10.81	284	
	322-482	5.59	332	
	482-1000	2.44	-	
	R.T.-1000	48.43	-	
A-Ce-MCM-Cl	R.T.-121	5.71	62	0.154
	121-283	22.74	245	
	283-312	2.48	304	
	312-350	2.72	-	
	350-452	8.54	395	
	452-1000	3.72	-	
A-Ce-MCM-NO ₃	R.T.-128	5.93	62	0.155
	128-291	22.77	249	
	291-317	2.37	309	
	317-358	3.06	-	
	358-494	8.60	400	
	494-1000	2.61	-	
	R.T.-1000	45.34	-	

Table S3. TGA results for the calcined MCM-41 materials.

Sample	Temperature range (°C)	Mass loss (%)	DTG maximum (°C)	Normalized silanol condensation mass loss (%)
Si-MCM-41	R.T.-118	4.58	58	1.70
	118-1000	1.62	-	
	R.T.-1000	6.20	-	
Ce-MCM-Cl	R.T.-148	14.23	76	3.50
	148-1000	3.00	-	
	R.T.-1000	17.23	-	
Ce-MCM-NO ₃	R.T.-128	12.29	67	2.67
	128-1000	2.34	-	
	R.T.-1000	14.63	-	

